Adaptive Multidimensional Fuzzy Sets for Texture Modeling

Pedro Manuel Martínez-Jiménez
Department of Automation, Electronics and Computer Architecture and Networks, University of Cádiz, Spain

Jesús Chamorro-Martínez
Department of Computer Science and Artificial Intelligence University of Granada, Spain

James M. Keller
Electrical Engineering and Computer Science Department, University of Missouri-Columbia, USA

This is the peer reviewed version of the following article: *Pedro Manuel Martínez-Jiménez, Jesús Chamorro-Martínez, James M. Keller: Adaptive multidimensional fuzzy sets for texture modeling. Int. J. Approx. Reasoning 103: 288-302 (2018)*, which has been published in final form at https://doi.org/10.1016/j.ijar.2018.10.006.

Abstract

The modeling of the perceptual properties of texture plays a fundamental role in tasks where some interaction with subjects is needed. In order to face the imprecision related to these properties, fuzzy sets defined on the domain of computational measures of the corresponding property are usually employed. In this sense, the most interesting approaches show that the combination of different measures as reference sets improve the texture characterization. However, the main drawback of these proposals is that they do not take into account the subjectivity associated with human perception. For example, the perception of a texture property may change depending on the user, and in addition, the image context may influence the global perception of a given property. In this paper, we propose to solve these problems by combining the use of several computational measures in a reference set with adaptation to the subjectivity of human perception. To do this, we propose a generic methodology that automatically transforms any multidimensional fuzzy set modeling a texture property to the particular perception of a new user or to the image

context. For this purpose, the information given by the user, or extracted from the textures present in the image, are employed.

Keywords: image analysis; texture modeling; human perception; adaptive models

1 Introduction

Texture is one of the most used low level features for image analysis and computer vision. In fact, since all the objects in nature have texture, its analysis plays a fundamental role in object or region recognition and classification [1, 2, 3]. An example of this importance can be appreciated in Figure 1, where several images with the same shape and a similar color are shown, but that can be identified thanks to the analysis of their texture.

There are many techniques in the literature for texture analysis, and the use of one or another depends on the particular task to which it is applied. In this sense, for a task where a textural description interpretable by humans is not needed, such as segmentation or texture classification, we can find many techniques that try to model texture by means of feature vectors. These approaches are based on genetic programming [4, 5], dictionary learning [6, 7], kernel learning [8, 9], Gabor functions [10, 11] or Wavelets [12, 13], and are considered as the golden standard in the literature.

However, in tasks where some interaction with subjects is needed, techniques with the ability of providing a perceptual texture characterization interpretable by humans can be more useful. In these approaches, texture is modeled on the basis of some vague textural properties that are usually employed by humans, like *coarseness*, *directionality*, *contrast*, *line-likeness* or *regularity* [14, 15, 16]. These perceptual properties are imprecise by nature, in the sense that, except in extreme cases, we cannot set a precise threshold between textures that exemplify a property and textures that do not. For example, we can reasonably say that the texture shown in Figure 2(a) is coarse and contrasted, and that the texture shown in Figure 2(c) is not, as they represent potential extreme cases for both properties. However, the fulfillment of these properties is not so clear for the texture shown in Figure 2(b). This way, the most interesting approaches arise from the fuzzy set field [17, 18, 19], as they are able to take into account the inherent uncertainty. In these proposals, a mapping from low-level statistical features (crisp computational measures of the corresponding property) to high level textural concepts is performed by defining membership functions for each texture feature.

In addition, it is widely known that the combination of different features in texture analysis improves its recognition and classification. In [20], several texture descriptors were evaluated both in isolation and by combining some of them by means of machine learning approaches. In that work, the authors concluded that certain selected texture measures play a complementary role to each other, satisfying that the combination of different features improves the classification accuracy. Similar studies were performed in [21] for unsupervised texture

(a) (b) (c)

Figure 1: Example of objects with the same shape and color, but different texture.

segmentation, demonstrating that the combination of features based on Gabor filters and the wavelet transform provides better performance compared to the individual features alone. In a similar way, we can find several approaches in the literature where the combination of different texture descriptors is applied to improve the accuracy in more specific tasks, such as breast density classification [22], cataract detection [23], meningioma subtype discrimination [24] or face recognition [25].

Focusing our analysis on the fuzzy approaches, two different groups can be found in the literature. In the first, each texture property is modeled as a whole by means of a unique fuzzy set, obtaining models that are able to directly represent the presence degree of that property [26, 27, 28]. In this type of approach the membership functions associated with the fuzzy sets are obtained by learning a functional relationship between the values given by the measures and the human perception of the property. In the second group, fuzzy partitions are proposed, providing a set of linguistic labels that are related to the presence degree of the property [29, 30, 31, 32]. In this case, the fuzzy partitions are generated through an unsupervised fuzzy clustering algorithm on the basis of the measured values obtained from an image database [31, 32], or by means of a distinguishability analysis applied to the measured values on the basis of the human perception of the texture property [29, 30]. Each group of fuzzy approaches provides a different way to represent the presence of the texture properties, and the use of one or another will depend on the task to which it is applied. The first group is useful in classical tasks like pattern recognition, while the second can be more useful in tasks where a texture characterization using linguistic terms is needed, such as semantic description of images or content-based image retrieval using linguistic queries.

Regarding the combination of texture features, most of the fuzzy approaches in the literature face this question by means of the use of subsets of measures as a reference set. This allows us to combine their abilities to capture the texture property, obtaining models that are able to represent this property with more fidelity. Since the membership functions associated with these fuzzy sets are defined in a domain of more than one dimension, they are referred to as mul-

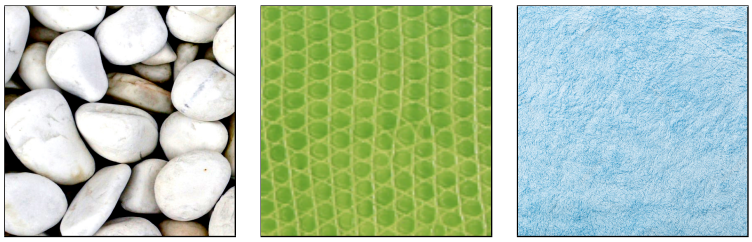

(a) (b) (c)

Figure 2: Examples showing the imprecision associated to the properties.

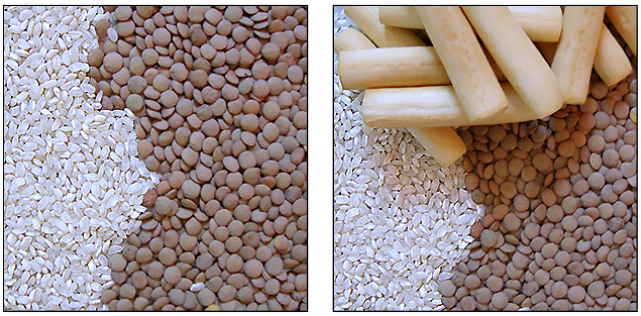

(a) (b)

Figure 3: Example showing the influence of the image context in the perception of the fineness property. The presence of the very coarse texture in (b) can inhibit the understanding of the rest of textures, and they may be perceived as finer than in (a). This figure has been taken from [28].

tidimensional models. Concerning this type of approach, an interesting study can be found in [27]. There, nineteen classical computational measures were analyzed and combined in pairs in order to model the properties of fineness, contrast and directionality. The performance of the obtained fuzzy models was evaluated according to human perception of the properties. Their conclusion was that the proposed bidimensional fuzzy models improve the characterization of the texture properties compared to the unidimensional fuzzy models in the literature. In addition, several experiments using these bidimensional models for pattern recognition were carried out, obtaining better results than those obtained with unidimensional models.

However, the main drawback of all these fuzzy approaches is that they do not take into account the subjectivity associated with human perception. On the one hand, the perception of a texture property may change depending on the person. For example, although we have considered that the texture shown

in Figure 2(a) is very coarse, another person may consider that this texture is not so coarse. On the other hand, image context may also affect the global perception of texture properties. An example of this fact can be seen in Figure 3. The images in figures 3(a) and 3(b) are very similar, but in the last one a new texture has been added. The presence of this texture, which is much coarser than the others, can inhibit the rest of the textures, and they may be perceived as finer than in Figure 3(a). Thus, context adaptation problem, which is a very important issue in practical applications nowadays [33, 34, 35, 36], should be also taken into account.

We can find several (crisp and fuzzy) approaches in the literature where the subjectivity associated with human perception has been considered for texture analysis. The majority of these proposals try to generate a corresponding model on the basis of human assessments [26, 31, 32], although they do not propose any technique for their later adaptation to new information, such as the particular perception of a person or to the image context. Regarding the techniques that try to adapt the model to the subjectivity of the human perception, two different groups can be distinguished. In the first group we can find the techniques referred as metric-based approaches [37, 38, 39], that are widely used in content-based image retrieval (CBIR). In this type of approach, user's feedback is employed to update weights in the metrics used to compute the similarity in the image features. However, the aim of these techniques is not to adapt the model itself (which remains static) but to adapt the importance of each feature in the similarity value.

In the second group, we find model-based approaches [40, 41, 42], which are the most interesting ones from the point of view of this paper. These approaches are usually focused on crisp techniques which use classifiers supporting a feedback stage, where the parameters are locally updated to adapt them to the particular perception of a person. Nevertheless, none of these approaches considers the imprecision inherent in the texture feature, as has been previously mentioned, and in addition they do not take into account the influence of the image context.

In this paper we propose to address both problems observed above, i.e. our aim is to combine i) the improvement in the texture modeling given by the use of a set of several computational measures, with ii) adaptation to the subjectivity of human perception. For this purpose, we propose a generic methodology that automatically adapts any multidimensional fuzzy model of a texture property to the particular perception of a person or to the image context. Starting from our preliminary work for the unidimensional case [28], in this paper we provide an adaptation method that is valid for any number of dimensions of the fuzzy model, i.e. any number of computational measures can be combined as a reference set. In this method, the membership functions associated with the fuzzy sets are automatically adapted by means of a functional transformation on the basis of the new perception. In order to take into account the particular perception of a new person, a set of texture images representing the particular profile of the person is employed in the transformation process. In the case of the adaptation to the image context, the information used in the transformation

process is obtained by analyzing the textures present in the image.

The rest of the paper is organized as follows. In section 2, a general overview of our methodology, as well as the used notation, are presented. The techniques proposed in this paper to obtain multidimensional fuzzy sets adapted to the perception of different users or to the image context are described in sections 3 and 4, respectively. In section 5 some results obtained by applying these models are shown, and the main conclusions are summarized in section 6.

2 Preliminaries and Notations

As mentioned in the previous section, several approaches can be found in the literature that try to model texture properties by means of fuzzy sets defined on the domain of computational measures of the corresponding property. The majority of these techniques propose only one measure for the reference set, but more recent approaches have shown that the combination of different computational measures improves texture characterization [27]. From now on, let $\mathcal{T}$ be one of these fuzzy sets modeling a texture property, defined on the domain of a given subset of n measures of this property (a multidimensional reference set), and whose membership function[1] is defined as

$$\mathcal{T} : \mathbb{R}^n \rightarrow [0, 1] \tag{1}$$

In addition, this membership function should satisfy the following conditions:

- The values $\mathcal{T}(\mathbf{x}) = 0$ and $\mathcal{T}(\mathbf{x}) = 1$ should be achievable for some feature vectors.
- The gradient of the function $\mathcal{T}$ must satisfy the following condition:

$$\|\nabla \mathcal{T}(\mathbf{x})\| \neq 0 \quad \forall \mathbf{x} \; / \; 0 < \mathcal{T}(\mathbf{x}) < 1 \tag{2}$$

In this scenario, given an image, a vector of measure values $\mathbf{M} = [m_1, \ldots, m_n]$ can be obtained from it, with m_j being the result of applying the j-th measure in the reference set to the image. This way, the presence of the texture property in this image can be estimated by using $\mathcal{T}$.

As has been mentioned in the previous section, the aim of this paper is to obtain adaptive fuzzy models that are able to represent the particular perception of a person. In our approach, we propose to obtain these models by adapting the generic fuzzy sets $\mathcal{T}$ described above. From now on, let $\tilde{\mathcal{T}} : \mathbb{R}^n \rightarrow [0, 1]$ be the adapted fuzzy set obtained from $\mathcal{T}$, that has the same reference set as $\mathcal{T}$ (the domain of the n computational measures of the property).

[1] To simplify the notation, as it is usual in the scope of fuzzy sets, we will use the same notation $\mathcal{T}$ for the fuzzy set and for the membership function that defines it.

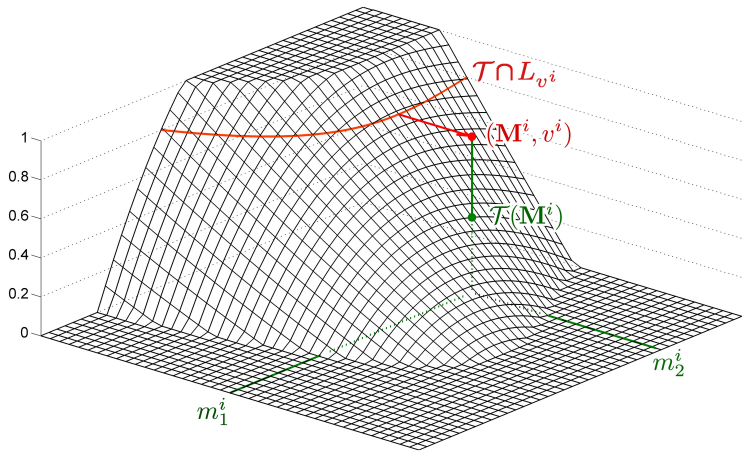

Figure 4: Graphical example of a non-adaptive fuzzy set $\mathcal{T}$ for $n = 2$, together with an adaptation point $(\mathbf{M}^i, v^i)$ and the intersection of the corresponding level set L_{v^i} with $\mathcal{T}$, i.e. $\mathcal{T} \cap L_{v^i}$.

3 Adaptation to User Profiles

Our adaptation approach for a certain membership function $\mathcal{T}$ is based on using information provided by users, specifically a collection $\mathcal{R} = \{R^1, \ldots, R^Z\}$ of texture images, $Z \geq 1$, each image having an associated presence degree of the corresponding property. Let $v^i \in [0, 1]$ be the degree provided for image R^i and let $\mathcal{V} = \{v^1, \ldots, v^Z\}$. We assume that the indexes are assigned so that $v^i < v^{i+1}$ (which also implies that no pair of images agree on the presence degree). Let also $\mathbf{M}^i = [m_1^i, \ldots, m_n^i]$ be a vector defined for each R^i as the collection of measures $m_j^i \in \mathbb{R}$ with $1 \leq j \leq n$ obtained by applying the j-th measure to R^i. Let us denote by $\mathcal{M} = \{\mathbf{M}^1, \ldots, \mathbf{M}^Z\}$ the set of feature vectors for $\mathcal{R}$. On this basis, we introduce what we call the *adaptation points* as the following ordered set:

$$\Omega = \{(\mathbf{M}^i, v^i)\}_{i=1,\ldots,Z} \tag{3}$$

with $\mathbf{M}^i \in \mathcal{M}$ and $v^i \in \mathcal{V}$, and with $v^i < v^{i+1}$ being the order relation.

These ideas are illustrated in Figure 4, where an adaptation point $(\mathbf{M}^i, v^i)$ is graphically depicted for $n = 2$, i.e. $\mathbf{M}^i = [m_1^i, m_2^i]$. The fuzzy model $\mathcal{T}$ corresponds to the surface shown in the figure, and the objective is to perform a suitable transformation of the surface so that the value of the function in $\mathbf{M}^i$ changes from $\mathcal{T}(\mathbf{M}^i)$ to v^i in a particular way that we explain below.

Our approach relies on the concept of a *level set*[2]. The level set of value v of the function $\mathcal{T}$ is

[2]The term *level set* is not employed here with the usual semantics of fuzzy set theory, but with the usual semantics employed in mathematics.

$$L_v(\mathcal{T}) = \{\mathbf{x} \in \mathbb{R}^n, \mathcal{T}(\mathbf{x}) = v\} \tag{4}$$

Depending on the number of measures, the level set is also known as *level curve* (for the case $n = 2$), *level surface* (for the case $n = 3$), and *level hypersurface* (for $n > 3$). An example is shown as a red curve in Figure 4, representing graphically the intersection of the level set for value v^i with $\mathcal{T}$. We also use the concepts of *lower level set* and *upper level set* to be $LL_v(\mathcal{T}) = \{\mathbf{x} \in \mathbb{R}^n, \mathcal{T}(\mathbf{x}) \leq v\}$ and $UL_v(\mathcal{T}) = \{\mathbf{x} \in \mathbb{R}^n, \mathcal{T}(\mathbf{x}) \geq v\}$, respectively. Finally, let us denote $L_v(\tilde{\mathcal{T}})$ by $\tilde{L}_v$ and $L_v(\mathcal{T})$ by L_v for simplicity. In the same spirit, for a given value $\mathbf{x} \in \mathbb{R}^n$, we use the inequalities $\mathbf{x} \leq \tilde{L}_v$ and $\mathbf{x} \geq \tilde{L}_v$ instead of the membership to the lower and the upper level sets $\mathbf{x} \in LL_v(\tilde{\mathcal{T}})$ and $\mathbf{x} \in UL_v(\tilde{\mathcal{T}})$, respectively.

The key role of level sets in our approach relies on the fact that the collection of all level sets for a certain $\mathcal{T}$ can be used as a representation of $\mathcal{T}$, similarly to the representation theorem of fuzzy sets based on alpha-cuts, since

$$\mathcal{T}(x) = v \text{ iff } x \in L_v(\mathcal{T}) \tag{5}$$

We use this representation in order to obtain $\tilde{\mathcal{T}}$ from $\mathcal{T}$ using the collection of adaptation points Ω in the following way: the level set $\tilde{L}_{v^i}$ with $v^i \in \mathcal{V}$ is obtained by performing multidimensional translation and expansion of the corresponding level set L_{v^i}. This transformation is performed so that $\mathbf{M}^i \in \tilde{L}_{v^i}$, and in such a way that for all the points $\mathbf{x} \in L_{v^i}$, their distance in the direction of the gradient of $\mathcal{T}$ in $\mathbf{x}$ to $L_{v^{i+1}}$ is reduced in a fixed proportion, given by the distance between $\mathbf{M}^i$ and the closest point in L_{v^i}. This is illustrated in Figure 5, and will be formalized in the next sections.

Note that computing all level sets $\tilde{L}_v$ for every $v \in [0, 1]$ extensively is not possible. Instead, the value of $\tilde{\mathcal{T}}(\mathbf{x})$ for any $\mathbf{x} \in \mathbb{R}^n$ is obtained on the basis of the original fuzzy set $\mathcal{T}$, and the level sets $\tilde{L}_{v^i}$ and $\tilde{L}_{v^{i+1}}$ that satisfy $\mathbf{x} \geq \tilde{L}_{v^i}$ and $\mathbf{x} \leq \tilde{L}_{v^{i+1}}$. For that purpose, a multidimensional translation and expansion function $\mathbf{A}_{\tilde{L}_{v^i}\tilde{L}_{v^{i+1}}}^{L_{v^i}L_{v^{i+1}}}(\mathbf{x})$ will be employed that basically computes a kind of inverse of the transformation performed when computing the level sets for the adapted function. The details of the calculation of $\tilde{\mathcal{T}}(\mathbf{x})$, that is intended to keep the proportions of the original function $\mathcal{T}$ in the transformed one, will also be explained and formalized in next sections.

It is important to remark that, for this approach to be feasible, the set Ω must satisfy an additional property: since the function $\tilde{\mathcal{T}}$ has to maintain the condition imposed by Equation (2) in this adaptation process, i.e. $\left\|\nabla\tilde{\mathcal{T}}(\mathbf{x})\right\| \neq 0 \quad \forall \mathbf{x} \,/\, 0 < \tilde{\mathcal{T}}(\mathbf{x}) < 1$, the adaptation points should satisfy the condition $\mathbf{M}^i \leq L_{v^{i+1}}$, that is, $\mathbf{M}^i$ must be in the lower level set $LL_{v^{i+1}}(\mathcal{T})$.

Formalizing these ideas, we propose to define $\tilde{\mathcal{T}}$ as a function of the form[3]

[3]Notice that the transformation for $\mathbf{x} \leq \tilde{L}_{v^1}$ and $\mathbf{x} \leq \tilde{L}_{v^2}$ is the same. In fact, as $\tilde{L}_{v^1} < \tilde{L}_{v^2}$ according to our notation, this condition can be reduced to $\mathbf{x} \leq \tilde{L}_{v^2}$. The same happens with $\mathbf{x} > \tilde{L}_{v^Z-1}$ and $\mathbf{x} > \tilde{L}_{v^Z}$, that can be reduced to $\mathbf{x} > \tilde{L}_{v^Z-1}$.

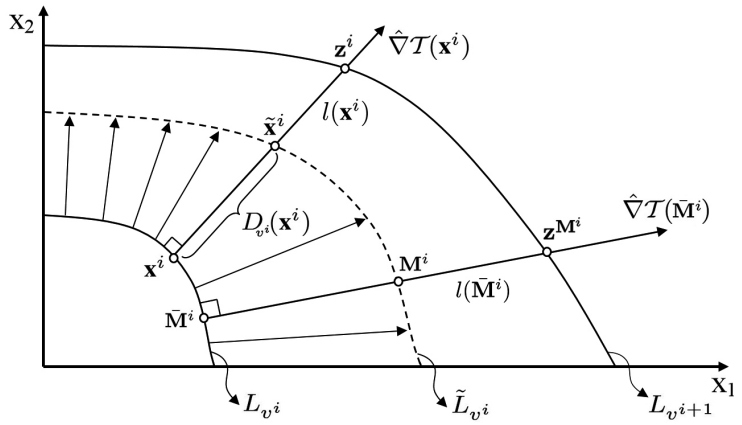

Figure 5: Graphical example of the parameters needed to calculate the level set $\tilde{L}_{v^i}$ for $n = 2$. Every point $\mathbf{x}^i$ in the original level set L_{v^i} is translated in the direction of the gradient of the original function ($\widehat{\nabla}\mathcal{T}(\mathbf{x}^i)$). The translation distance $D_{v^i}(\mathbf{x}^i)$ is proportional to the separation between the level sets L_{v^i} and $L_{v^{i+1}}$.

$$\tilde{\mathcal{T}}(\mathbf{x};\Omega) = \begin{cases} \mathcal{T}(\mathbf{A}^{L_{v^1} L_{v^2}}_{\tilde{L}_{v^1} \tilde{L}_{v^2}}(\mathbf{x})) & \mathbf{x} \leq \tilde{L}_{v^1} \; or \; \mathbf{x} \leq \tilde{L}_{v^2}, \\ \vdots & \\ \mathcal{T}(\mathbf{A}^{L_{v^i} L_{v^{i+1}}}_{\tilde{L}_{v^i} \tilde{L}_{v^{i+1}}}(\mathbf{x})) & \tilde{L}_{v^i} < \mathbf{x} \leq \tilde{L}_{v^{i+1}}, \\ \vdots & \\ \mathcal{T}(\mathbf{A}^{L_{v^Z-1} L_{v^Z}}_{\tilde{L}_{v^Z-1} \tilde{L}_{v^Z}}(\mathbf{x})) & \mathbf{x} > \tilde{L}_{v^Z-1} \; or \; \mathbf{x} > \tilde{L}_{v^Z} \end{cases} \tag{6}$$

In the next sections we are going to explain in detail the remaining aspects of our proposal: (i) how the level sets $\tilde{L}_{v^i}, i = 1, \ldots, Z$ of the adapted model are obtained (section 3.1), (ii) how to determine $\mathbf{x} \leq \tilde{L}_{v^i}$ and $\mathbf{x} \geq \tilde{L}_{v^i}$ (section 3.2) and (iii) how the functions $\mathbf{A}^{L_{v^i} L_{v^{i+1}}}_{\tilde{L}_{v^i} \tilde{L}_{v^{i+1}}}(\mathbf{x})$ are defined (section 3.3).

3.1 Calculating the Level Sets $\tilde{L}_{v^i}$

Our approach for computing $\tilde{L}_{v^i}$ for any $n > 0$ is illustrated in Figure 5 for $n = 2$. Level curves of values v^i and v^{i+1} of the original model are represented by solid lines, whilst the adapted curve $\tilde{L}_{v^i}$ is depicted as a dashed line. The transformation translates every point $\mathbf{x}^i$ in the original level sets in the direction of the gradient of the original function in that point as follows:

$$\tilde{\mathbf{x}}^i = \mathbf{x}^i + D_{v^i}(\mathbf{x}^i)\widehat{\nabla}\mathcal{T}(\mathbf{x}^i) \tag{7}$$

with $\widehat{\nabla}\mathcal{T}(\mathbf{x}^i)$ being the unit vector in the direction of the gradient in $\mathbf{x}^i$. The translation distance $D_{v^i}(\mathbf{x}^i)$ is proportional to the separation between the level sets L_{v^i} and $L_{v^{i+1}}$ in the direction of the gradient. Let $l(\mathbf{x}^i)$ be the line that goes through the point $\mathbf{x}^i$ and has the same direction as the gradient in this point. Let $\mathbf{z}^i$ be the intersection of $L_{v^{i+1}}$ and $l(\mathbf{x}^i)$ (see Figure 5). Then

$$D_{v^i}(\mathbf{x}^i) = K_{v^i} \cdot \left\|\mathbf{x}^i - \mathbf{z}^i\right\| \tag{8}$$

where K_{v^i} is calculated as follows: let $\bar{\mathbf{M}}^i \in L_{v^i}$ be that point in L_{v^i} whose gradient goes through $\mathbf{M}^i$, i.e. the point that is translated to $\mathbf{M}^i$ in the transformation (both lying on $l(\bar{\mathbf{M}}^i)$). Note that $\mathbf{M}^i$ is the only known point that must reside on $\tilde{L}_{v^i}$. Let $\mathbf{z}^{\mathbf{M}^i}$ be the intersection of $L_{v^{i+1}}$ and $l(\bar{\mathbf{M}}^i)$. Then

$$K_{v^i} = \frac{\left\|\mathbf{M}^i - \bar{\mathbf{M}}^i\right\|}{\left\|\bar{\mathbf{M}}^i - \mathbf{z}^{\mathbf{M}^i}\right\|} \tag{9}$$

Note that K_{v^i} is the same for all the points of the level set L_{v^i}. This proportionality is used in Equation (8) to transform the entire level set L_{v^i} into $\tilde{L}_{v^i}$.

3.2 Solving the Inequalities $\mathbf{x} < \tilde{L}_{v^i}$ and $\mathbf{x} > \tilde{L}_{v^i}$

As introduced in previous sections, $\mathbf{x} < \tilde{L}_{v^i}$ and $\mathbf{x} > \tilde{L}_{v^i}$ stand for $\tilde{\mathcal{T}}(\mathbf{x}) < v^i$ and $\tilde{\mathcal{T}}(\mathbf{x}) > v^i$, respectively. The main problem is that $\tilde{\mathcal{T}}(\mathbf{x})$ is not known in general; of the function $\tilde{\mathcal{T}}$ we just know the level sets $\tilde{L}_{v^i}$.

Given a point $\mathbf{x}$, let $\mathbf{p}^i \in L_{v^i}$ be the point in L_{v^i} whose gradient goes through $\mathbf{x}$, that is, the point in L_{v^i} closest to $\mathbf{x}$.

Let $\tilde{\mathbf{p}}^i \in \tilde{L}_{v^i}$ be the point in $\tilde{L}_{v^i}$ where $\mathbf{p}^i$ has been translated according to the methodology described in the previous section. Note that $\mathbf{p}^i$, $\tilde{\mathbf{p}}^i$, and $\mathbf{x}$ lie on the same line, the direction of which is defined by the gradient $\widehat{\nabla}\mathcal{T}(\mathbf{p}^i)$. Thus, the inequality $\mathbf{x} > \tilde{L}_{v^i}$ holds iff the sense of the vector that goes from $\tilde{\mathbf{p}}^i$ to $\mathbf{x}$ matches that of $\widehat{\nabla}\mathcal{T}(\mathbf{p}^i)$, i.e.

$$\mathbf{x} > \tilde{L}_{v^i} \quad iff \quad \widehat{\tilde{\mathbf{p}}^i\mathbf{x}} = \widehat{\nabla}\mathcal{T}(\mathbf{p}^i) \tag{10}$$

Similarly,

$$\mathbf{x} < \tilde{L}_{v^i} \quad iff \quad \widehat{\tilde{\mathbf{p}}^i\mathbf{x}} = -\widehat{\nabla}\mathcal{T}(\mathbf{p}^i) \tag{11}$$

3.3 Defining the Function $\mathbf{A}^{L_{v^i}L_{v^{i+1}}}_{\tilde{L}_{v^i}\tilde{L}_{v^{i+1}}}(\mathbf{x})$

As can be seen in Equation (6), in order to calculate the value of the adapted membership function $\tilde{\mathcal{T}}$ in a point $\mathbf{x}$, the idea is to find the point $\mathbf{A}(\mathbf{x})$ translated to $\mathbf{x}$ in the adaptation. The value of $\mathcal{T}$ for such point will be the value of $\tilde{\mathcal{T}}$ for $\mathbf{x}$.

Since $\tilde{\mathcal{T}}$ is defined as a piecewise function, the function $\mathbf{A}$ varies depending on the level sets enclosing $\mathbf{x}$, and hence it is denoted as $\mathbf{A}^{L_{v^i}L_{v^{i+1}}}_{\tilde{L}_{v^i}\tilde{L}_{v^{i+1}}}$.

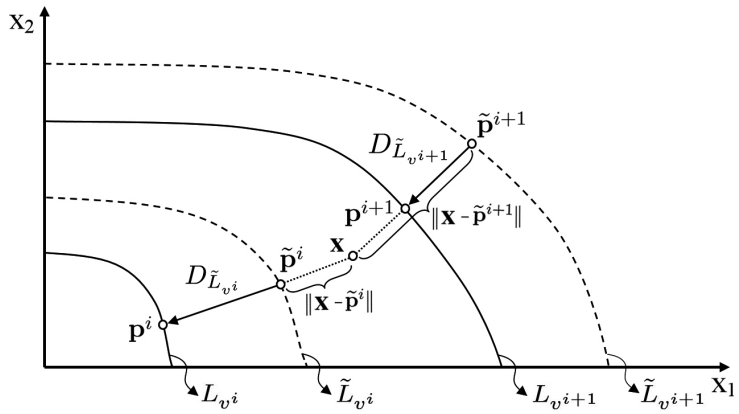

Figure 6: Graphical example of the parameters needed to calculate the proposed transformation for $n = 2$. Given a point $\mathbf{x}$, with $\tilde{L}_{v^i} \leq \mathbf{x} \leq \tilde{L}_{v^{i+1}}$, its transformation will be a combination of the translations of the level sets $\tilde{L}_{v^i}$ and $\tilde{L}_{v^{i+1}}$ ($D_{\tilde{L}_{v^i}}$ and $D_{\tilde{L}_{v^{i+1}}}$) weighted by the relative distances from $\mathbf{x}$ to $\tilde{L}_{v^{i+1}}$ and $\tilde{L}_{v^i}$ ($RD(\mathbf{x}, \tilde{L}_{v^{i+1}})$ and $RD(\mathbf{x}, \tilde{L}_{v^i})$).

Before going into details, let us point out that the main requirement for $\mathbf{A}^{L_{v^i} L_{v^{i+1}}}_{\tilde{L}_{v^i} \tilde{L}_{v^{i+1}}}$ is that, for every point $\mathbf{x} \in \tilde{L}_{v^i}$, the function must yield the corresponding point in L_{v^i}. This way, if we know $\tilde{L}_{v^i}$ for all $v \in [0, 1]$, the function is exactly the inverse of the transformation.

Figure 6 shows a graphical example where we can see all the parameters needed to calculate the proposed transformation for $n = 2$. Let us suppose that we want to calculate the transformation of a given point $\mathbf{x} \in \mathbb{R}^n$, with $\tilde{L}_{v^i} \leq \mathbf{x} \leq \tilde{L}_{v^{i+1}}$. Let us also suppose that the level set $\tilde{L}_{v^i}$ is translated to L_{v^i} and that $\tilde{L}_{v^{i+1}}$ is translated to $L_{v^{i+1}}$ (note that these are the inverse of the translation applied in section 3.1 to obtain the level sets $\tilde{L}_{v^i}$ from L_{v^i}).

According to the notation of the previous section, let $\mathbf{p}^i \in L_{v^i}$ and $\mathbf{p}^{i+1} \in L_{v^{i+1}}$ be the point in each level set L_{v^i} and $L_{v^{i+1}}$ with the minimum Euclidean distance to $\mathbf{x}$. Let also $\tilde{\mathbf{p}}^i \in \tilde{L}_{v^i}$ and $\tilde{\mathbf{p}}^{i+1} \in \tilde{L}_{v^{i+1}}$ be the points where $\mathbf{p}^i$ and $\mathbf{p}^{i+1}$ have been translated to by using equation (7)[4]. This way, the translations of the level sets $\tilde{L}_{v^i}$ and $\tilde{L}_{v^{i+1}}$ can be calculated as $D_{\tilde{L}_{v^i}} = (\mathbf{p}^i - \tilde{\mathbf{p}}^i)$ and $D_{\tilde{L}_{v^{i+1}}} = (\mathbf{p}^{i+1} - \tilde{\mathbf{p}}^{i+1})$, respectively. In addition, we can calculate the relative distances from $\mathbf{x}$ to $\tilde{L}_{v^i}$ and $\tilde{L}_{v^{i+1}}$ as

$$RD(\mathbf{x}, \tilde{L}_{v^i}) = \frac{\left\|\mathbf{x} - \tilde{\mathbf{p}}^i\right\|}{\left\|\mathbf{x} - \tilde{\mathbf{p}}^i\right\| + \left\|\mathbf{x} - \tilde{\mathbf{p}}^{i+1}\right\|} \tag{12}$$

[4]Note that they are also the points of $\tilde{L}_{v^i}$ and $\tilde{L}_{v^{i+1}}$ with the minimum Euclidean distance to $\mathbf{x}$.

$$RD(\mathbf{x}, \tilde{L}_{v^{i+1}}) = \frac{\left\|\mathbf{x} - \tilde{\mathbf{p}}^{i+1}\right\|}{\left\|\mathbf{x} - \tilde{\mathbf{p}}^{i}\right\| + \left\|\mathbf{x} - \tilde{\mathbf{p}}^{i+1}\right\|} \tag{13}$$

Thus, given a point $\mathbf{x}$, with $\tilde{L}_{v^i} \leq \mathbf{x} \leq \tilde{L}_{v^{i+1}}$, we propose a transformation of the form:

$$\begin{aligned}
\mathbf{A}_{\tilde{L}_{v^i}\tilde{L}_{v^{i+1}}}^{L_{v^i}L_{v^{i+1}}}(\mathbf{x}) &= \mathbf{x} \; + RD(\mathbf{x}, \tilde{L}_{v^{i+1}}) D_{\tilde{L}_{v^i}} + RD(\mathbf{x}, \tilde{L}_{v^i}) D_{\tilde{L}_{v^{i+1}}} \\
&= \mathbf{x} \; + \frac{\left\|\mathbf{x} - \tilde{\mathbf{p}}^{i+1}\right\|}{\left\|\mathbf{x} - \tilde{\mathbf{p}}^{i}\right\| + \left\|\mathbf{x} - \tilde{\mathbf{p}}^{i+1}\right\|} \left(\mathbf{p}^i - \tilde{\mathbf{p}}^i\right) \\
&\quad + \frac{\left\|\mathbf{x} - \tilde{\mathbf{p}}^{i}\right\|}{\left\|\mathbf{x} - \tilde{\mathbf{p}}^{i}\right\| + \left\|\mathbf{x} - \tilde{\mathbf{p}}^{i+1}\right\|} \left(\mathbf{p}^{i+1} - \tilde{\mathbf{p}}^{i+1}\right)
\end{aligned} \tag{14}$$

It can be noticed that the translation of $\mathbf{x}$ will be a combination of the translations of the level sets $\tilde{L}_{v^i}$ and $\tilde{L}_{v^{i+1}}$ ($D_{\tilde{L}_{v^i}}$ and $D_{\tilde{L}_{v^{i+1}}}$) weighted by the relative distances from $\mathbf{x}$ to $\tilde{L}_{v^{i+1}}$ and $\tilde{L}_{v^i}$ ($RD(\mathbf{x}, \tilde{L}_{v^{i+1}})$ and $RD(\mathbf{x}, \tilde{L}_{v^i})$). Note that, if $x \in \tilde{L}_{v^i}$ (i.e. $x = \tilde{\mathbf{p}}^i$), then $RD(\mathbf{x}, \tilde{L}_{v^i}) = 0$ and $RD(\mathbf{x}, \tilde{L}_{v^{i+1}}) = 1$. This implies that $\mathbf{A}_{\tilde{L}_{v^i}\tilde{L}_{v^{i+1}}}^{L_{v^i}L_{v^{i+1}}}(\mathbf{x}) = x + D_{\tilde{L}_{v^i}} = \mathbf{p}^i$, i.e. x will be translated to the corresponding point in L_{v^i}, as it was expected. In a similar way, if $x \in \tilde{L}_{v^{i+1}}$, its transformation is given by the translation of the level set $\tilde{L}_{v^{i+1}}$, i.e. $\mathbf{A}_{\tilde{L}_{v^i}\tilde{L}_{v^{i+1}}}^{L_{v^i}L_{v^{i+1}}}(\mathbf{x}) = \mathbf{p}^{i+1}$.

3.4 Particular Case of $Z = 1$

We have to take into account that equation (6) is valid only for $Z > 1$. In the particular case of $Z = 1$ only a translation is needed. In this case $\Omega = \{(\mathbf{M}^1, v^1)\}$, which implies that the level set L_{v^1} should be translated to go through the point $\mathbf{M}^1$. Figure 7 shows an example of the case $Z = 1$ for $n = 2$. As has been mentioned in the previous sections, the translation of each point $\mathbf{x}^1 \in L_{v^1}$ will be performed in the direction of its gradient, transforming it into the point $\tilde{\mathbf{x}}^1 \in \tilde{L}_{v^1}$ according to equation (7). In order to calculate the translation distance $D_{v^1}(\mathbf{x}^1)$ using equation (8), we propose this distance to be proportional to the separation between the level sets L_{v^i} and $L_{v^{i+1}}$ in each direction. However, in this case, the level set $L_{v^{i+1}}$ does not exist, so we need to choose a different reference level set, e.g. L_1 (the level set where the model takes the value 1).

As in the previous section, let's suppose that the level set $\tilde{L}_{v^1}$ is translated to L_{v^1} (the inverse of the translation applied to obtain the level set $\tilde{L}_{v^1}$ from L_{v^1} according to the methodology proposed in section 3.1). Given a point $\mathbf{x} \in \mathbb{R}^n$, it has been translated in the same direction and distance as the points in $\tilde{L}_{v^1}$. Following the same notation as in previous sections, let $\mathbf{p}^1 \in L_{v^1}$ be the point in the level set L_{v^1} with the minimum Euclidean distance to $\mathbf{x}$ (and whose gradient direction goes through $\mathbf{x}$) and let $\tilde{\mathbf{p}}^1 \in \tilde{L}_{v^1}$ be the point in $\tilde{L}_{v^1}$ where $\mathbf{p}^1$ has

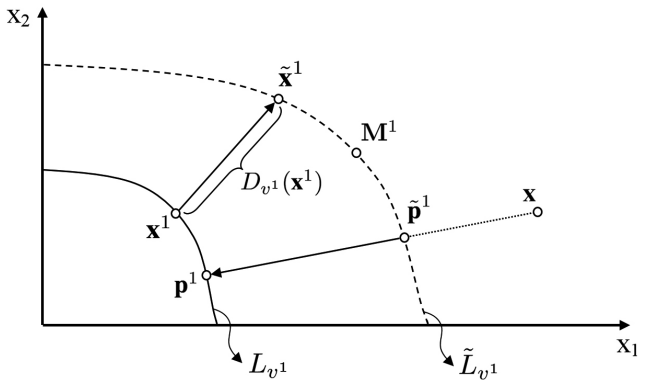

Figure 7: Example of $Z = 1$ for $n = 2$. In this case, only one level set L_{v^1} (and the corresponding level set $\tilde{L}_{v^1}$ of the adapted function) is employed. Given a point $\mathbf{x}$, only a translation in the same direction and distance as the points in $\tilde{L}_{v^1}$ will be applied, i.e. the same translation as $\tilde{\mathbf{p}}^1$.

been translated to by using equation (7). The translation applied to $\mathbf{x}$ will be performed in the same direction and distance as $\tilde{\mathbf{p}}^1$, and it has the form

$$\tilde{\mathcal{T}}(\mathbf{x}; \Omega) = \mathcal{T}(\mathbf{x} + (\mathbf{p}^1 - \tilde{\mathbf{p}}^1)) \tag{15}$$

4 Adaptation to Image Context

Natural images will usually show several textures with different perception degrees of the properties. It is natural to assume that the textures with the minimum and the maximum presence of a property in the image may influence the perception of this property for the rest of textures, i.e. the perception can depend on the context. For example, in the case of the fineness property, the coarsest and the finest texture in the image may inhibit the rest of textures, influencing their perception of fineness, as it is shown in Figure 3.

In this section, a proposal for adapting the membership function $\mathcal{T}$ to the image context is presented. In our approach, the minimum and the maximum perception degrees of the property in the model, i.e. the values of the reference set where the function $\tilde{\mathcal{T}}$ achieves the membership degrees 0 and 1, will depend on the inhibition present in the image. In turn, this inhibition will depend on the difference between the textures with the minimum and the maximum presence of the property in the image, in the sense that the greater this difference, the stronger the inhibition.

From now on, let $\mathbf{M}^{min}$ and $\mathbf{M}^{max}$ be the vector of measure values obtained by applying the computational measures in the reference set to the textures with the minimum and the maximum presence of the property in the image, respectively; let λ be the inhibition degree present in the image for the corresponding

property; and let $\mathbf{M}^0$ and $\mathbf{M}^1$ be the values of the reference set that will impose the minimum and the maximum perception degrees of $\tilde{\mathcal{T}}$, respectively. At this point, our first aim is to obtain the values $\mathbf{M}^{min}$ and $\mathbf{M}^{max}$ of the corresponding image. Secondly, these values will be used to estimate the inhibition degree λ. Finally, this inhibition degree will be used to calculate the adaptation points $\mathbf{M}^0$ and $\mathbf{M}^1$. This way, the membership function $\tilde{\mathcal{T}}$ adapted to the image context can be obtained by applying the same transformation shown in section 3 on the basis of the set $\Omega = \{(\mathbf{M}^0, 0), (\mathbf{M}^1, 1)\}$.

In order to obtain the textures with the minimum and the maximum presence of the property in the image, for each pixel in the original image, the values of the measures in the reference set are calculated using a window centered at this pixel. Let $\mathcal{M} = \{\mathbf{M}_i,\ \mathbf{M}_i \leq \mathbf{M}_{i+1}\}_{i=1,\ldots,N}$ be the ordered set of the measure vectors calculated from the N pixels in the image. Since the values obtained with different measures are not comparable, in order to perform this ranking we will take into account only the value of one of the measures in the reference set[5]. In particular, in this paper we propose to rank the vectors in $\mathcal{M}$ according to the measure that better captures the presence of the texture property (the measure with the highest goodness value according to the studies in [27]), although a different criterion may be employed. Thus, we will consider that $\mathbf{M}_i \leq \mathbf{M}_{i+1}$ if $m_{k,i} \leq m_{k,i+1}$, with P_k being the measure with the highest goodness value.

The textures with the minimum and the maximum presence of the property will correspond with the first and the last element in $\mathcal{M}$, respectively[6], i.e. $\mathbf{M}^{min} = \mathbf{M}_1$ and $\mathbf{M}^{max} = \mathbf{M}_N$. However, in order to avoid the influence of outliers (the presence of very low and very large measure values), the elements $z > 1$ and $z' < N$ have been chosen, i.e. $\mathbf{M}^{min} = \mathbf{M}_z$ and $\mathbf{M}^{max} = \mathbf{M}_{z'}$. In particular, we propose to use the 20^{th} percentile and the 80^{th} percentile in $\mathcal{M}$, i.e. $z = round(0.2N + 0.5)$ and $z' = round(0.8N + 0.5)$, with $round(x)$ being the function that returns the nearest integer to x.

Once the values $\mathbf{M}^{min}$ and $\mathbf{M}^{max}$ are calculated, the next step is to estimate the inhibition degree λ present in the image. In this paper, we consider that λ will reach the highest degree ($\lambda = 1$) if the difference $\left|\mathbf{M}^{max} - \mathbf{M}^{min}\right|$ is *large enough*, and it will decrease as this difference is smaller. However, as we have commented above, the values obtained with different measures are not comparable, so we propose to calculate this difference by using the measure considered to rank the vectors in $\mathcal{M}$ (in our case, the measure that better captures the presence of the texture property). Thus, we propose to define the inhibition degree as a value between 0 and 1 of the form

$$\lambda = \begin{cases} \frac{\left|m_k^{max} - m_k^{min}\right|}{U_k} & \left|m_k^{max} - m_k^{min}\right| < U_k, \\ 1 & \left|m_k^{max} - m_k^{min}\right| \geq U_k \end{cases} \tag{16}$$

[5]Note that in this case there are no presence degrees of the corresponding property associated to these images to perform the ranking, as in the adaptation to user profiles. In addition, we can not use $\mathcal{T}$ to estimate the presence of the texture property in these images, because this function saturates at 0 and 1.

[6]For a measure P_k that increases according to the perception of the property.

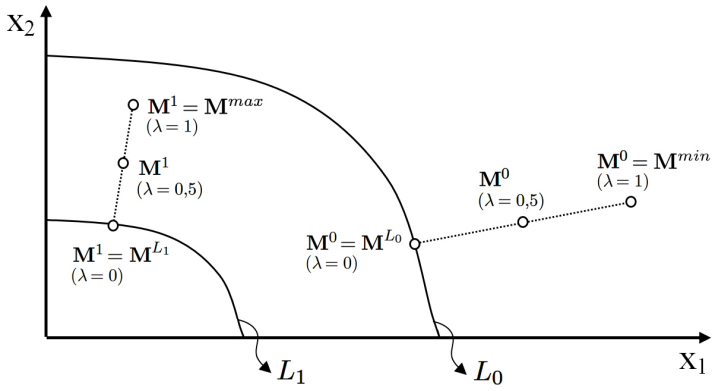

Figure 8: Graphical example of $\mathbf{M}^0$ and $\mathbf{M}^1$ in the adaptation to the image context for $n = 2$ and the inhibition degrees $\lambda = 1$, $\lambda = 0.5$ and $\lambda = 0$.

with $m_k^{max} \in \mathbf{M}^{max}$ and $m_k^{min} \in \mathbf{M}^{min}$ being the elements in $\mathbf{M}^{max}$ and $\mathbf{M}^{min}$ corresponding to the measure P_k with the highest goodness value, and with U_k being the threshold value for considering that the difference between the textures with the maximum and the minimum presence of the property in the image is large enough[7].

At this point, the aim is to obtain $\mathbf{M}^0$ and $\mathbf{M}^1$ on the basis of the inhibition degree. Figure 8 shows a graphical example of $\mathbf{M}^0$ and $\mathbf{M}^1$ for the inhibition degrees $\lambda = 1$, $\lambda = 0.5$ and $\lambda = 0$. In our approach, if the inhibition is strong ($\lambda = 1$), $\mathbf{M}^0$ and $\mathbf{M}^1$ will be imposed by the textures with the minimum and the maximum presence of the property in the image, i.e. $\mathbf{M}^0 = \mathbf{M}^{min}$ and $\mathbf{M}^1 = \mathbf{M}^{max}$, respectively. On the contrary, if no inhibition is present in the image ($\lambda = 0$), $\mathbf{M}^0$ and $\mathbf{M}^1$ will coincide with the corresponding values of the non-adaptive model, i.e. the points where $\mathcal{T}$ takes the values 0 and 1, respectively. However, as it was commented in section 3, there are infinite points where these values are reached: the level sets L_0 and L_1. From now on, let $\mathbf{M}^{L_0} \in L_0$ and $\mathbf{M}^{L_1} \in L_1$ be the points in L_0 and L_1 whose gradient goes through $\mathbf{M}^{min}$ and $\mathbf{M}^{max}$, respectively. As these are the point in L_0 and L_1 with the lowest euclidean distance to $\mathbf{M}^{min}$ and $\mathbf{M}^{max}$, they can be calculated by solving the following minimization problem

$$\mathbf{M}^{L_0} = \underset{\mathbf{x}^0 \in L_0}{\arg\min} \left\| \mathbf{x}^0 - \mathbf{M}^{min} \right\| \tag{17}$$

$$\mathbf{M}^{L_1} = \underset{\mathbf{x}^1 \in L_1}{\arg\min} \left\| \mathbf{x}^1 - \mathbf{M}^{max} \right\| \tag{18}$$

Thus, we propose to calculate $\mathbf{M}^0$ and $\mathbf{M}^1$ as

$$\mathbf{M}^0 = \mathbf{M}^{L_0} + \lambda \cdot (\mathbf{M}^{min} - \mathbf{M}^{L_0}) \tag{19}$$

[7]Note that this threshold value will depend on the measure P_k.

$$\mathbf{M}^1 = \mathbf{M}^{L_1} + \lambda \cdot (\mathbf{M}^{max} - \mathbf{M}^{L_1}) \tag{20}$$

This way, if no inhibition is present in the image ($\lambda = 0$), $\mathbf{M}^0 = \mathbf{M}^{L_0}$ and $\mathbf{M}^1 = \mathbf{M}^{L_1}$, so the non-adaptive model is not affected by the adaptation to the image context, as expected. As the inhibition increases, $\mathbf{M}^0$ will gradually take values in the line that goes from $\mathbf{M}^{L_0}$ to $\mathbf{M}^{min}$, reaching this last value for the maximum inhibition degree ($\lambda = 1$). In a similar way, $\mathbf{M}^1$ will take the values in the line that goes from $\mathbf{M}^{L_1}$ to $\mathbf{M}^{max}$, as it is shown in Figure 8.

5 Results

In this section, several experiments using the proposed adaptation method are shown. In the first three experiments, fuzzy sets adapted to the particular perception of different users are described, analyzing their ability to represent the corresponding profile. The last experiment shows an example where the fuzzy sets are adapted to the image context, analyzing their ability to represent the perception of the texture properties influenced by the context.

For the first experiment, we considered Figure 9(a), corresponding to a microscopic image of a volvox, which is a colony of greencells. In this image we can see the main colony, composed of numerous flagellate cells embedded in a semitransparent gelatinous ball, as well as 7 daughter colonies growing up inside it (the green spheres). Note that several textures with different perceptual degrees of fineness are shown, corresponding to the background, the main colony, and the daughter colonies. Figure 9(d) shows a mapping from the original image to its fineness values using the bidimensional non-adaptive model proposed in [27], corresponding to the pair of measures $\{FD, Amadasun\}$. For each pixel in the original image, a centered window of size 32×32 has been analyzed and its fineness membership degree has been calculated using the fuzzy model. This degree has been mapped into a gray level from 0 to 255. It can be noticed that this mapping represents the fineness of the different textures present in the image according to the average fineness perception gathered from the poll: a fine texture (pixels in white) corresponding to the daughter colonies, an intermediate coarseness texture (pixels with an intermediate grey level) corresponding to the main colony, and a coarse texture (pixels in black) corresponding to the background.

Now we modify the non-adaptive model to the fineness perception of two users. In this case, both users give a feedback about the fineness presence of the texture in the subimage surrounded by a white square in Figure 9(a) according to their particular perception. Specifically, it contains the texture of the main colony, that has an intermediate fineness perception according to the non-adaptive model (a fineness membership degree around 0.5). However, it is perceived as a very fine texture (membership degree 1) by the *user 1*, and as a very coarse texture (membership degree 0) by the *user 2*, as it is shown in figures 9(b) and 9(c).

Figures 9(e) and 9(f) show a mapping from the original image to its fineness values using the model adapted to the particular perception of the *user 1* and

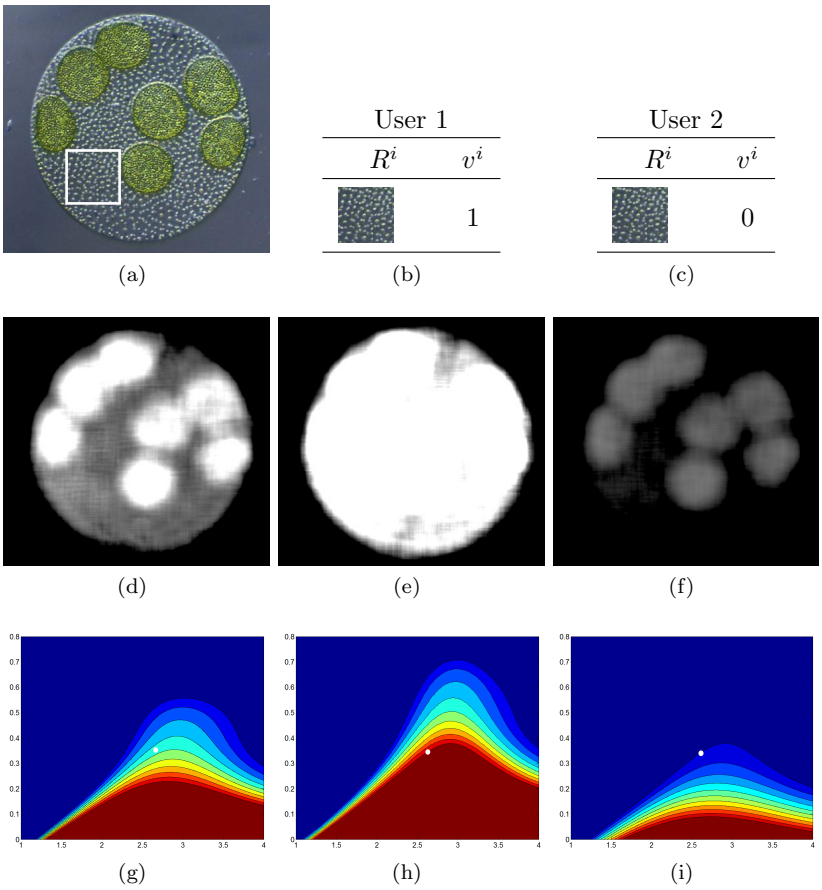

Figure 9: Results for the fineness property. (a) Original image. (b)(c) Samples representing the particular fineness perception of two different users. (d) Mapping from the original image to its fineness values using the non-adaptive model. (e)(f) Mapping using the fuzzy model adapted to *user 1* and *user 2*, respectively. (g) Top view of the non-adaptive model. (h)(i) Top view of the fuzzy model adapted to *user 1* and *user 2*, respectively.

the *user 2*, respectively. It can be noticed that, in the first case, the main colony, as well as the daughter colonies, are considered very fine, which is in accordance with the fineness perception of *user 1*. In the second case, the main colony, as well as the background, is considered very coarse, while the daughter colonies have an intermediate fineness degree. This is also in accordance with the particular perception of *user 2*, who considers all textures are coarser than the average.

Figures 9(g)-(i) display a 2D graphical representation (top view) of the non-

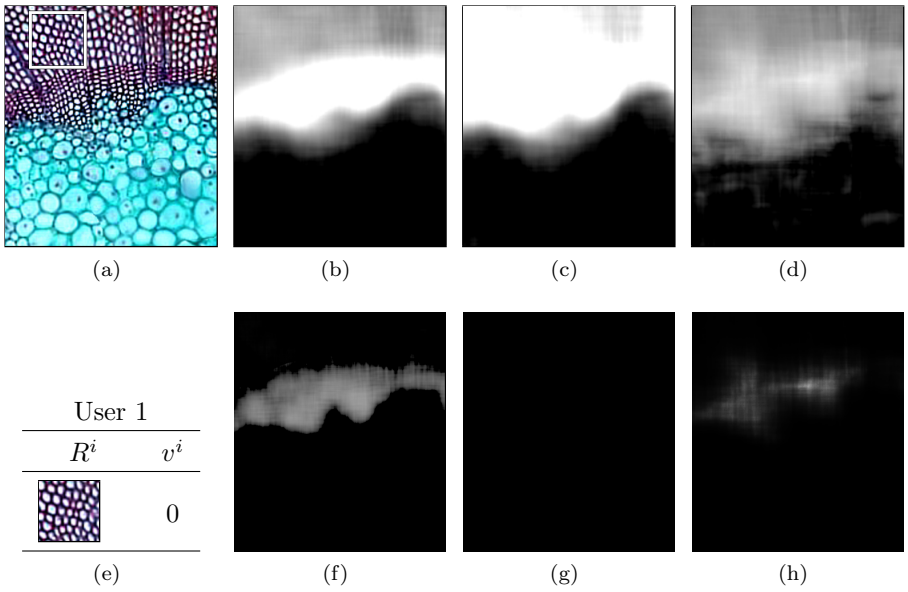

Figure 10: Results for the fineness property. (a) Original image. (b) Mapping from the original image to its fineness values using the proposed bidimensional non-adaptive model, corresponding to the pair of measures $\{FD, Amadasun\}$. (c)(d) Mapping using the unidimensional non-adaptive models proposed in [28] for each measure separately (Amadasun (c) and FD (d)). (e) Samples representing the particular fineness perception of a user. (f)(g)(h) Mapping using the fuzzy models employed in (b)(c)(d) adapted to the user, respectively.

adaptive model, and the model adapted to the particular perception of *user 1* and *user 2*, respectively. The two dimensions in the depiction correspond to the two measures employed as reference set, while the colors are related to the membership degrees, representing 10 different levels from 0 (dark blue) to 1 (dark red) in steps of 0.1. The measures used as the reference set have been applied to the sample image given by the users, and the obtained values have been represented as a white point in the figures (this is the adaptation point in both cases). It can be noticed that, according to the proposed methodology, the level curve L_1 in the adaptation to the first user, and the level curve L_0 in the adaptation to the second one, have been forced to go through this adaptation point.

In the second experiment, we compare the approach proposed in this paper with the work in [28], where unidimensional adaptive models where introduced. In this experiment, we considered Figure 10(a), corresponding to a microscopic image of plant cells, where several textures with different perceptual degrees of fineness are shown. Figure 10(b) shows a mapping from the original image to

its fineness values using the proposed bidimensional non-adaptive model, corresponding to the pair of measures $\{FD, Amadasun\}$. As in the first experiment, it can be noticed that this mapping represents the fineness of the different textures present in the image according to the average fineness perception gathered from the poll: a coarse texture (pixels in black) corresponding to the big cells at the bottom of the image, an intermediate coarseness texture (pixels with an intermediate grey level) corresponding to the intermediate size cells at the top of the image, and a fine texture (pixels in white) corresponding to the small cells between them.

Figures 10(c) and 10(d) show a mapping using the unidimensional non-adaptive models proposed in [28] for the measures of Amadasun and FD, respectively. It can be noticed that in this case, the unidimensional models are not able to capture the fineness degree of the textures present in the image. This way, multidimensional models should be used to improve the texture characterization, and, in order to adapt them to the subjectivity of human perception, the adaptive multidimensional fuzzy approach proposed in this paper is needed. In fact, Figures 10(f)-(h) show a mapping from the original image using the fuzzy models adapted to the particular perception of a user. As in the previous experiment, the user gives a feedback about the fineness presence of the texture in the subimage surrounded by a white square in Figure 10(a). Specifically, it contains the texture of the intermediate size cells, that has an intermediate fineness perception according to the non-adaptive model. However, it is perceived as a very coarse texture (membership degree 0) by the user, as it is shown in Figure 10(e). It can be noticed that, using the bidimensional adaptive model (Figure 10(f)), the intermediate size cells, as well as the big cells, are considered as very coarse, while the small cells have an intermediate fineness degree, which is in accordance with the particular perception of the user. However, using the unidimensional adaptive models (Figures 10(g) and 10(h)), the results do not match with this perception. Thus, in this experiment we have shown that i) the combination of different computational measures as reference set improves the texture characterization, and ii) the method proposed in this paper improves the unidimensional adaptive fuzzy approaches.

For the third experiment, we considered Figure 11(a), corresponding to a natural image where several textures with different perceptual degrees of contrast are shown. Figure 11(c) shows a mapping from the original image to its contrast values using the bidimensional non-adaptive model proposed in [27], corresponding to the pair of measures $\{Tamura, Haralick\}$. As in the previous experiment, it can be noticed that this mapping represents the contrast presence according to the average contrast perception: a high contrasted texture (pixels in white) corresponding to the leopard skin, a low contrasted texture (pixels in black) corresponding to the background, and a half-contrasted texture (pixels with an intermediate gray level) corresponding to the branch. Finally, Figure 11(d) shows the original image using this mapping as alpha channel. It can be noticed that the contrasted region corresponding to the leopard skin emerge with ease, while the region of the branch is a bit transparent, and the background has disappeared completely.

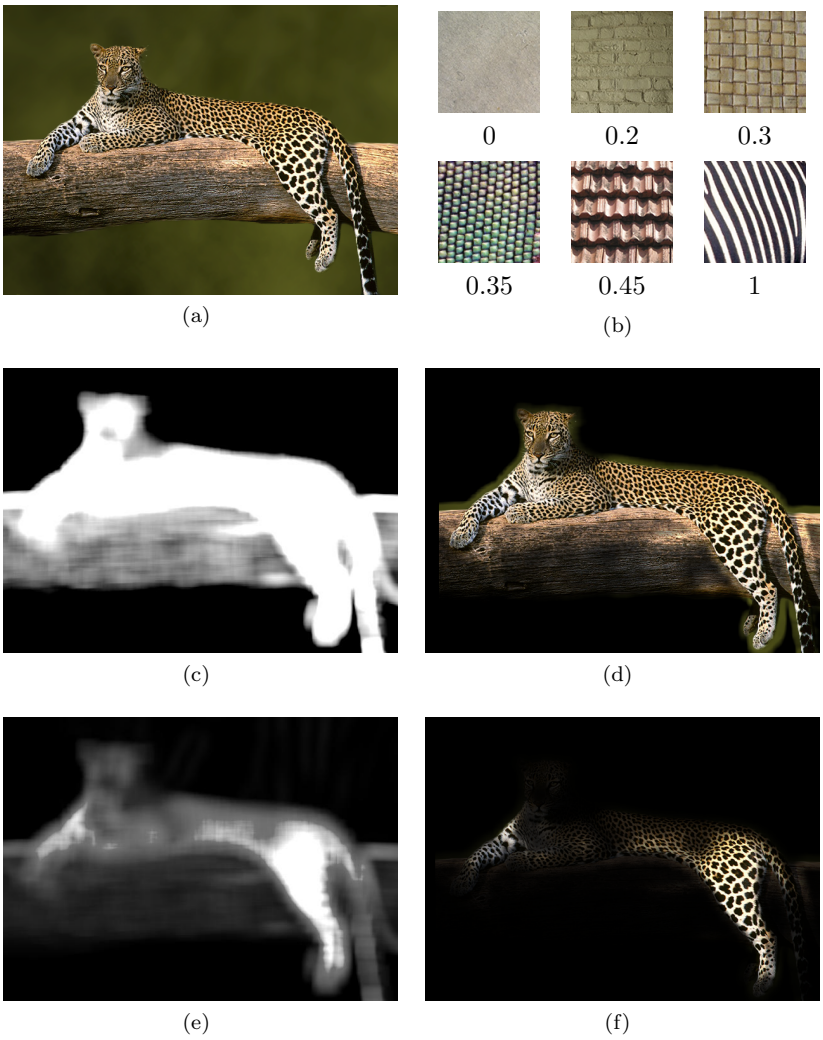

Figure 11: Results for the contrast property. (a) Original image. (b) Samples representing the particular contrast perception of a user. (c) Mapping from the original image to its contrast values using the non-adaptive model. (e) Mapping using the fuzzy model adapted to the user. (d)(f) Original image using the mappings in (c) and (e) as alpha channel, respectively.

Now let's modify the non-adaptive model to the particular contrast perception of a user. Figure 11(b) shows six texture images given by this user to represent his/her particular perception, each one with an associated presence degree of contrast. The three textures in the second row are considered as very contrasted according to the non-adaptive model. However, only the last one is

perceived by this user as a very contrasted texture (membership degree 1), while the membership degrees given to the other two are 0.35 and 0.45, respectively. Figure 11(e) shows a mapping from the original image in Figure 11(a) to its contrast values using the adapted model. It can be seen that in this case all the leopard skin is not considered as a very contrasted texture, but only the legs, where the skin is white and the spots are more salient. The rest of the body is now considered as a low contrasted texture, which is in accordance with the contrast perception of this user. Figure 11(f) shows the original image using this mapping as alpha channel. It can be noticed that in this case the legs of the leopard emerge with ease, while the rest of the body has almost disappeared, as well as the branch and the background.

Figure 12 presents an example where the non-adaptive fineness model is adapted to the image context. For this experiment, we have considered Figure 12(a), corresponding to a microscopic image of a corneal cell. Figure 12(b) shows a mapping from the original image to its fineness values using the bidimensional non-adaptive model proposed in [27], corresponding to the pair of measures $\{FD, Amadasun\}$. It can be noticed that the texture of the cell nucleus, that is much finer than the other textures in the image, is considered as very fine according to the non-adaptive model. Now let's consider Figure 12(d), which is a zoom of a section of the image shown in Figure 12(a). The corresponding mapping using the non-adaptive model is shown in Figure 12(e). It can be noticed that, due to the absolute nature of the non-adaptive model, the obtained degrees depend on the zoom level of the image. Thus, in this case the texture of the nucleus is not considered as very fine.

The adaptation to the image context proposed in this paper can be used to reduce the influence of the zoom level. In order to calculate the inhibition degree λ, for this experiment we have used the measure of $Amadasun$, that according to [27] is the measure in the reference set that better captures the fineness presence. In this case, we propose to apply a threshold value $U_k = |\alpha - \beta|$, with α and β being the values defined in [27] (the values where the unidimensional model corresponding to the measure of $Amadasun$ achieves the fineness degrees 1 and 0, respectively).

Figures 12(c) and 12(f) show a mapping from the images in figures 12(a) and 12(d) using the model adapted to the corresponding image context. It can be noticed that, since the value where $\tilde{\mathcal{T}}$ achieves the fineness degree 1 depends on the finest texture in the image, the region corresponding to the cell nucleus is considered as a very fine texture in both mappings. Thus, the influence of the zoom level has been reduced, and the obtained results are in accordance with the change in the fineness perception due to the image context.

6 Conclusions and Future Works

In this paper, an adaptive multidimensional fuzzy approach has been proposed to model perceptual properties of texture. We combined adaptation to the subjectivity of a human's perception with the improvement in the texture char-

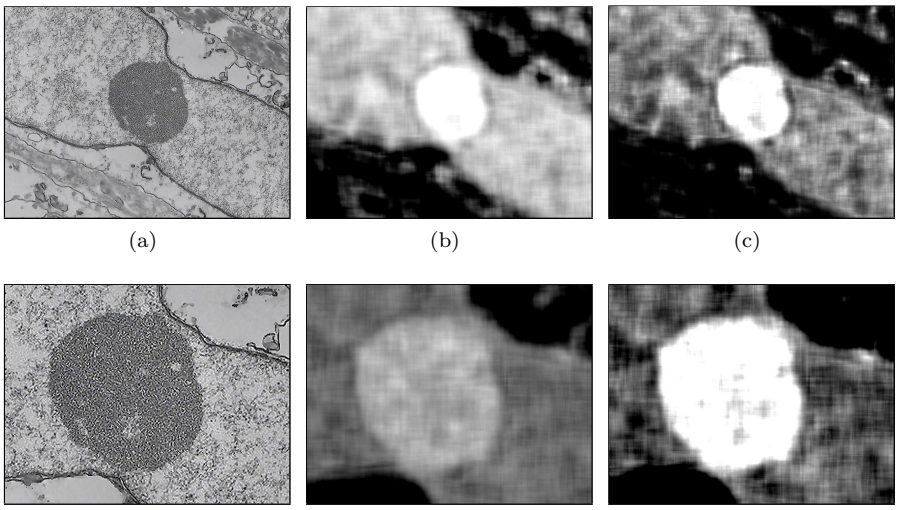

Figure 12: Adaptation to the image context for the fineness property. (a)(d) Original images. (b)(e) Mapping from the original images to their fineness values using the non-adaptive model. (c)(f) Mapping using the fuzzy model adapted to the image context.

acterization given by the combination of different computational measures as a reference set. Some experiments have been performed in order to analyze the ability of the adapted models obtained with the proposed methodology to represent different perceptions of given texture properties. In particular, in the experiments shown in section 5, the bidimensional fuzzy sets proposed in our previous work [27] have been used, although the proposed adaptation method is valid for any other fuzzy sets that represent the presence degree of texture properties. In these experiments we have shown that, in the case of the adaptation to users' profiles, the perception degrees provided by the obtained models match what each particular user would expect. In addition, in the case of the adaptation to the image context, we have shown that the obtained models are able to represent the perception of the texture properties influenced by the context.

The proposed approach can be very useful in applications where a perceptual texture characterization is employed, and, in particular, in tasks that need some interaction with subjects, where the subjectivity of human's perception may be an important issue. For example, it can be applied in expert systems, where the information provided by the expert is related to the presence of the texture properties. In this case, the perception of a texture property may change depending on the field of application: the concept of "very fine" may be different for a geologist, who analyzes satellite images, than for a medical expert, who study the textures present in x-ray or microscopic images. Moreover, even in the

same field of application, two experts may have different perceptions about the texture properties. Thus, using the adaptive multidimensional fuzzy approach proposed in this paper, the systems can be adapted to the particular perception of the corresponding expert.

In addition, the proposed approach can be used for context-awareness in different applications, such as semantic description of images or segmentation. In particular, it can be employed in order to reduce the influence of the zoom level in segmentation tasks, as has been shown in the last experiment of section 5.

In this work, several lines of research have been left open. First, although we have focused our study on membership functions $\mathcal{T}$ satisfying Equation (2), we are working on a solution to apply the proposed methodology with functions that do not satisfy this condition. Second, we will take into account the possibility of inconsistencies in the images given by subjects to represent his particular perception. And finally, we will extend the proposed methodology to other image features that can be modeled by a fuzzy set $\mathcal{T}$ satisfying the imposed conditions, such as fuzzy colors.

Acknowledgments

This work has been partially supported by the Spanish Ministry of Economy and Competitiveness and the European Regional Development Fund - ERDF (Fondo Europeo de Desarrollo Regional - FEDER) under project TIN2014-58227-P. We also would like to thank Dr. Daniel Sánchez for his valuable assistance in the field of fuzzy logic.

References

[1] E. Davies, Machine Vision: Theory, Algorithms, Practicalities, Morgan Kaufmann Publishers Inc., San Francisco, CA, USA, 2004.

[2] M. Jian, L. Liu, F. Guo, Texture image classification using perceptual texture features and gabor wavelet features, in: Proceedings of the Asia-Pacific Conference on Information Processing, Vol. 2, IEEE Computer Society, 2009, pp. 55–58.

[3] B. S. Manjunath, W. Y. Ma, Texture features for browsing and retrieval of image data, IEEE Transactions on Pattern Analysis and Machine Intelligence 18 (8) (1996) 837–842.

[4] L. Shao, L. Liu, X. Li, Feature learning for image classification via multiobjective genetic programming, IEEE Transactions on Neural Networks and Learning Systems 25 (7) (2014) 1359–1371.

[5] P. Srisook, K. Praditwong, Automatic feature weight assignment based on image retrieval using genetic algorithm, Advanced Materials Research 931-932 (2014) 1402–1406.

[6] Y. Gao, R. Ji, W. Liu, Q. Dai, G. Hua, Weakly supervised visual dictionary learning by harnessing image attributes, IEEE Transactions on Image Processing 23 (12) (2014) 5400–5411.

[7] F. Zhu, L. Shao, Weakly-supervised cross-domain dictionary learning for visual recognition, International Journal of Computer Vision 109 (1-2) (2014) 42–59.

[8] D. Cheng, T. Sun, X. Jiang, A robust image classification scheme with sparse coding and multiple kernel learning, in: Digital Forensics and Watermaking, Vol. 7809 of Lecture Notes in Computer Science, Springer Berlin Heidelberg, 2013, pp. 520–529.

[9] J. Li, Y. Wang, S. Chu, J. F. Roddick, Kernel self-optimization learning for kernel-based feature extraction and recognition, Information Sciences 257 (2014) 70–80.

[10] Z. Huang, S. Lo, N. Mayr, W. Yuh, Texture segmentation in magnetic resonance images using discrete wavelet transform combined with gabor wavelets, Medical Physics 40 (2013) 175.

[11] A. G. Zuñiga, J. B. Florindo, O. M. Bruno, Gabor wavelets combined with volumetric fractal dimension applied to texture analysis, Pattern Recognition Letters 36 (2014) 135–143.

[12] S. Hu, C. Xu, W. Guan, Y. Tang, Y. Liu, Texture feature extraction based on wavelet transform and gray-level co-occurrence matrices applied to osteosarcoma diagnosis, Bio-Medical Materials and Engineering 24 (1) (2014) 129–143.

[13] N. E. Lasmar, Y. Berthoumieu, Gaussian copula multivariate modeling for texture image retrieval using wavelet transforms, IEEE Transactions on Image Processing 23 (5) (2014) 2246–2261.

[14] M. Amadasun, R. King, Textural features corresponding to textural properties, IEEE Transactions on Systems, Man and Cybernetics 19 (5) (1989) 1264–1274.

[15] R. C. Gonzalez, R. E. Woods, Digital Image Processing, 2nd Edition, Prentice Hall, 2002.

[16] H. Tamura, S. Mori, T. Yamawaki, Textural features corresponding to visual perception, IEEE Transactions on Systems, Man and Cybernetics 8 (1978) 460–473.

[17] H. Aboulmagd, N. El-Gayar, H. Onsi, A new approach in content-based image retrieval using fuzzy, Telecommunication Systems 40 (1) (2009) 55–66.

[18] D. Antonypandiarajan, K. Suganya, Performance analysis for coal texture classification, in: Proceedings of the 2012 International Conference on Emerging Trends in Science, Engineering and Technology, Tiruchirappalli, India, 2012, pp. 251–254.

[19] S. Kulkarni, B. Verma, Fuzzy logic based texture queries for CBIR, in: Proceedings of the 5th International Conference on Computational Intelligence and Multimedia Applications, Xi'an, China, 2003, pp. 223–228.

[20] A. Barley, C. Town, Combinations of feature descriptors for texture image classification, Journal of Data Analysis and Information Processing 2 (3) (2014) 67–76.

[21] S. Rao, M. Puri, S. Das, Unsupervised segmentation of texture images using a combination of Gabor and wavelet features, in: Proceedings of the Fourth Indian Conference on Computer Vision, Graphics & Image Processing, 2004, pp. 370–375.

[22] G. Liasis, C. Pattichis, S. Petroudi, Combination of different texture features for mammographic breast density classification, in: 2012 IEEE 12th International Conference on Bioinformatics Bioengineering (BIBE), 2012, pp. 732–737.

[23] Y. Fuadah, A. Setiawan, T. Mengko, Budiman, Mobile cataract detection using optimal combination of statistical texture analysis, in: 2015 4th International Conference on Instrumentation, Communications, Information Technology, and Biomedical Engineering (ICICI-BME), 2015, pp. 232–236.

[24] O. Al-Kadi, Texture measures combination for improved meningioma classification of histopathological images, Pattern Recognition 43 (6) (2010) 2043 – 2053.

[25] S. Rahman, S. M. Naim, A. A. Farooq, M. Islam, Combination of Gabor and curvelet texture features for face recognition using principal component analysis, International Journal of Computer & Electrical Engineering 4 (3).

[26] J. Chamorro-Martínez, P. Martínez-Jiménez, J. Soto-Hidalgo, B. Prados-Suárez, Perception-based fuzzy sets for visual texture modelling, Soft Computing 18 (12) (2014) 2485–2499.

[27] J. Chamorro-Martínez, P. Martínez-Jiménez, J. Soto-Hidalgo, A. León-Salas, A fuzzy approach for modelling visual texture properties, Information Sciences 313 (1) (2015) 1–21.

[28] J. Chamorro-Martínez, P. Martínez-Jiménez, J. Soto-Hidalgo, B. Prados-Suárez, An adaptive fuzzy approach for modelling visual texture properties, Fuzzy Sets and Systems 286 (2016) 86–113.

[29] J. Chamorro-Martínez, P. Martínez-Jiménez, J. Soto-Hidalgo, Fuzzy partitions for modelling texture properties: Coarseness, contrast and directionality, in: IEEE International Conference on Fuzzy Systems, Istambul (Turkey), 2015, pp. 1–8.

[30] P. Martínez-Jiménez, J. Chamorro-Martínez, J. Soto-Hidalgo, Fuzzy partitions for texture modelling adapted to the subjectivity of human perception, in: 2016 IEEE International Conference on Fuzzy Systems (FUZZ-IEEE), 2016, pp. 1105–1112.

[31] H. C. Lin, C. Y. Chiu, S. N. Yang, Finding textures by textual descriptions, visual examples, and relevance feedbacks, Pattern Recognition Letters 24 (14) (2003) 2255–2267.

[32] A.-Z. Shih, The approach of using fractal dimension and linguistic descriptors in CBIR, in: Proceedings of the 2012 International Conference on Machine Learning and Cybernetics, Vol. 5, Shaanxi, China, 2012, pp. 1704–1707.

[33] U. Alegre, J. Augusto, T. Clark, Engineering context-aware systems and applications: A survey, Journal of Systems and Software 117 (2016) 55–83.

[34] J. Cadenas, N. Marín, M. Vila, Context-aware fuzzy databases, Applied Soft Computing 25 (2014) 215–233.

[35] M. Madkour, D. E. Ghanami, A. Maach, A. Hasbi, Context-aware service adaptation: An approach based on fuzzy sets and service composition, Journal of Information Science and Engineering 29 (1) (2013) 1–16.

[36] M. Sohn, S. Jeong, H. Lee, Case-based context ontology construction using fuzzy set theory for personalized service in a smart home environment, Soft Computing 18 (9) (2014) 1715–1728.

[37] Y. Rui, T. Huang, M. Ortega, S. Mehrotra, Relevance feedback: a power tool for interactive content-based image retrieval, IEEE Transactions on Circuits and Systems for Video Technology 8 (5) (1998) 644–655.

[38] M. Yasmin, S. Mohsin, M. Sharif, Intelligent image retrieval techniques: A survey, Journal of Applied Research and Technology 12 (1) (2014) 87 – 103.

[39] J. Yue, Z. Li, L. Liu, Z. Fu, Content-based image retrieval using color and texture fused features, Mathematical and Computer Modelling 54 (3-4) (2011) 1121 – 1127.

[40] J. Kress, S. Xu, G. Tourassi, A novel graphical user interface for high-efficacy modeling of human perceptual similarity opinions, in: Proceedings SPIE Medical Imaging, Vol. 8673, 2013, pp. 867306–867306–11.

[41] M. Schroder, H. Rehrauer, K. Seidel, M. Datcu, Interactive learning and probabilistic retrieval in remote sensing image archives, IEEE Transactions on Geoscience and Remote Sensing 38 (5) (2000) 2288–2298.

[42] J. Wang, H. Jing, M. Wernick, R. Nishikawa, Y. Yang, Analysis of perceived similarity between pairs of microcalcification clusters in mammograms, Medical Physics 41 (5) (2014) 051904.